Supporting Information

Resonant level and band splitting boost the thermoelectric performance of p-type polycrystalline SnSe

Chunlu Wu,[1] Xiao-Lei Shi,[2,] Meng Li,[2] Wei-Di Liu,[2] Daohao Li,[3] Liangkui Zhu,[4] Pei Yuan,[5] Zhuanghao Zheng,[1,*] Lina Cheng,[6,*] Zhi-Gang Chen,[2,*] and Xiangdong Yao[7]*

[1] Shenzhen Key Laboratory of Advanced Thin Films and Applications, Key Laboratory of Optoelectronic Devices and Systems of Ministry of Education and Guangdong Province, State Key Laboratory of Radio Frequency Heterogeneous Integration, College of Physics and Optoelectronic Engineering, Shenzhen University, Shenzhen, Guangdong, 518060, China

[2] School of Chemistry and Physics, ARC Research Hub in Zero-emission Power Generation for Carbon Neutrality, and Centre for Materials Science, Queensland University of Technology, Brisbane, Queensland 4000, Australia

[3] State Key Laboratory of Bio-fibers and Eco-textiles, College of Materials Science and Engineering, Qingdao University, Qingdao 266071, China

[4] State Key Laboratory of Inorganic Synthesis and Preparative Chemistry, College of Chemistry, Jilin University, Changchun 130012, China

[5] College of Materials Science and Engineering, Fuzhou University, Fuzhou 350002, China

[6] Institute of Green Chemistry and Molecular Engineering (IGCME), Sun Yat-sen University, Guangzhou, Guangdong 510275, China

[7] School of Advanced Energy and IGCME, Shenzhen Campus, Sun Yat-Sen University (SYSU), Shenzhen 518107, China

E-mail: xiaolei.shi@qut.edu.au (X.-L. Shi), zhengzh@szu.edu.cn (Z. Zheng), l.n.cheng@hotmail.com (L. Cheng), zhigang.chen@qut.edu.au (Z.-G. Chen)

1. Supporting figures

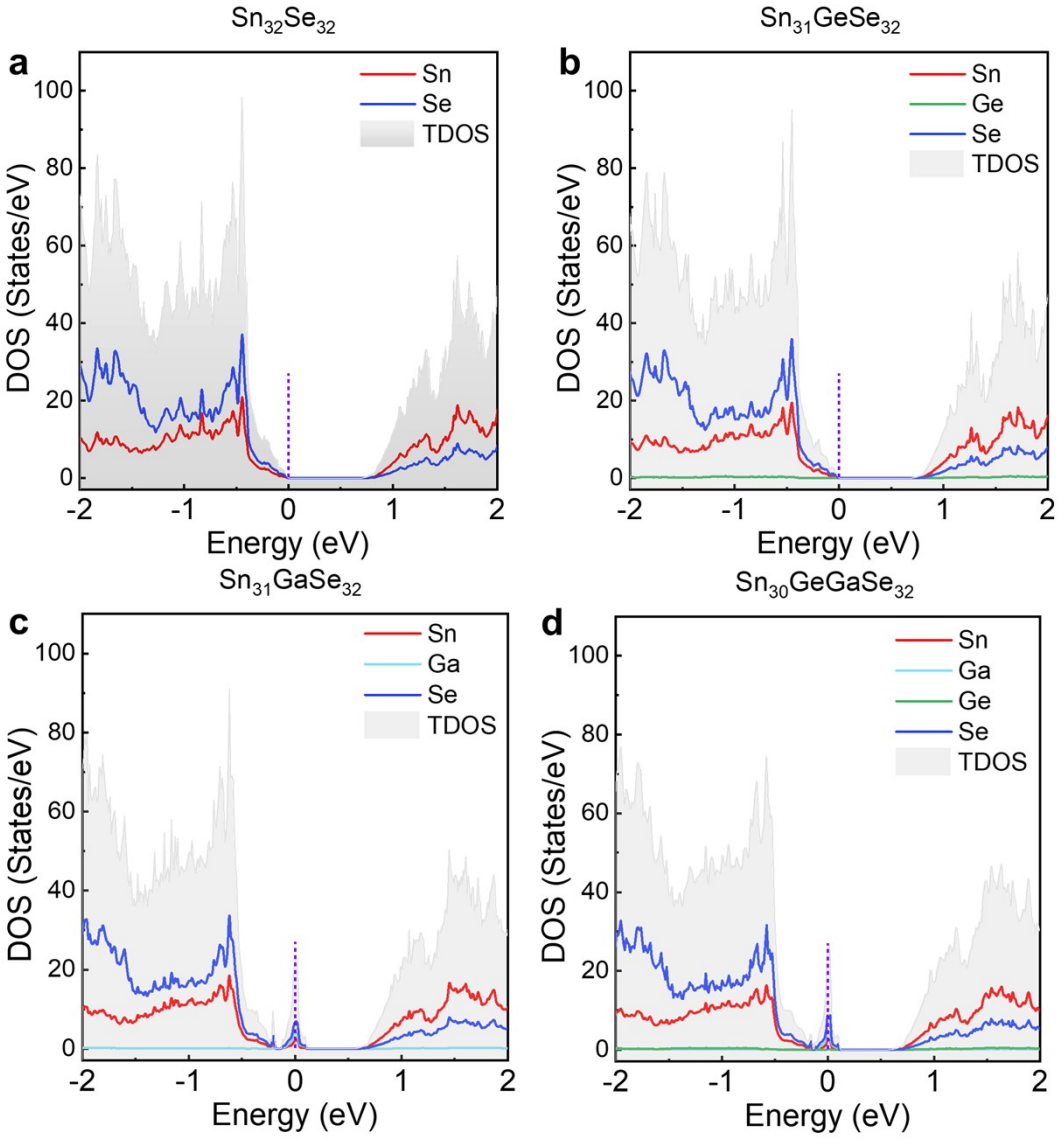

Figure S1. Computed partial and total density of states plots. (a) $Sn_{32}Se_{32}$, (b) $Sn_{31}GeSe_{32}$, (c) $Sn_{31}GeSe_{32}$, and (d) $Sn_{30}GeGaSe_{32}$.

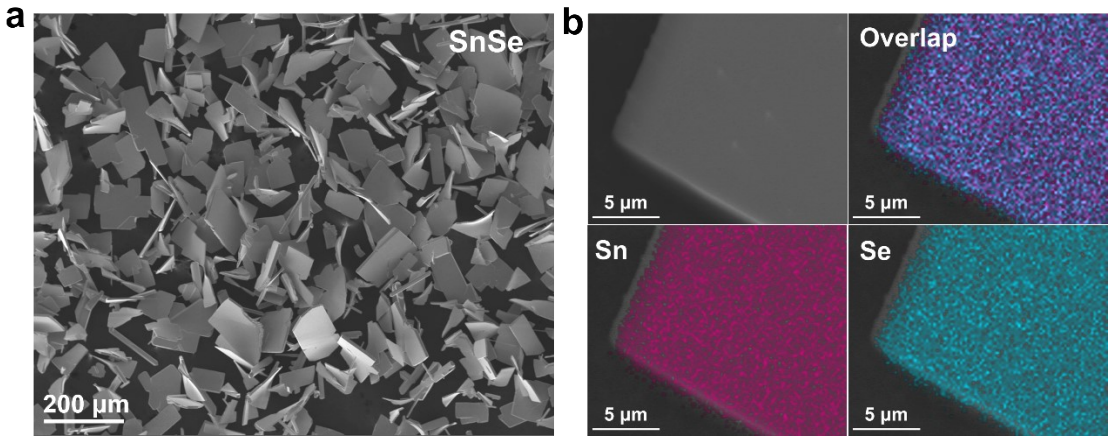

Figure S2. Scanning electron microscopy (SEM) and energy dispersive X-ray spectrometry (EDS) results of pure SnSe powders. (a) SEM image of undoped SnSe powder. (b) Enlarged SEM image of a SnSe microplate and corresponding EDS maps, including the overlapped and individual Sn and Se elements.

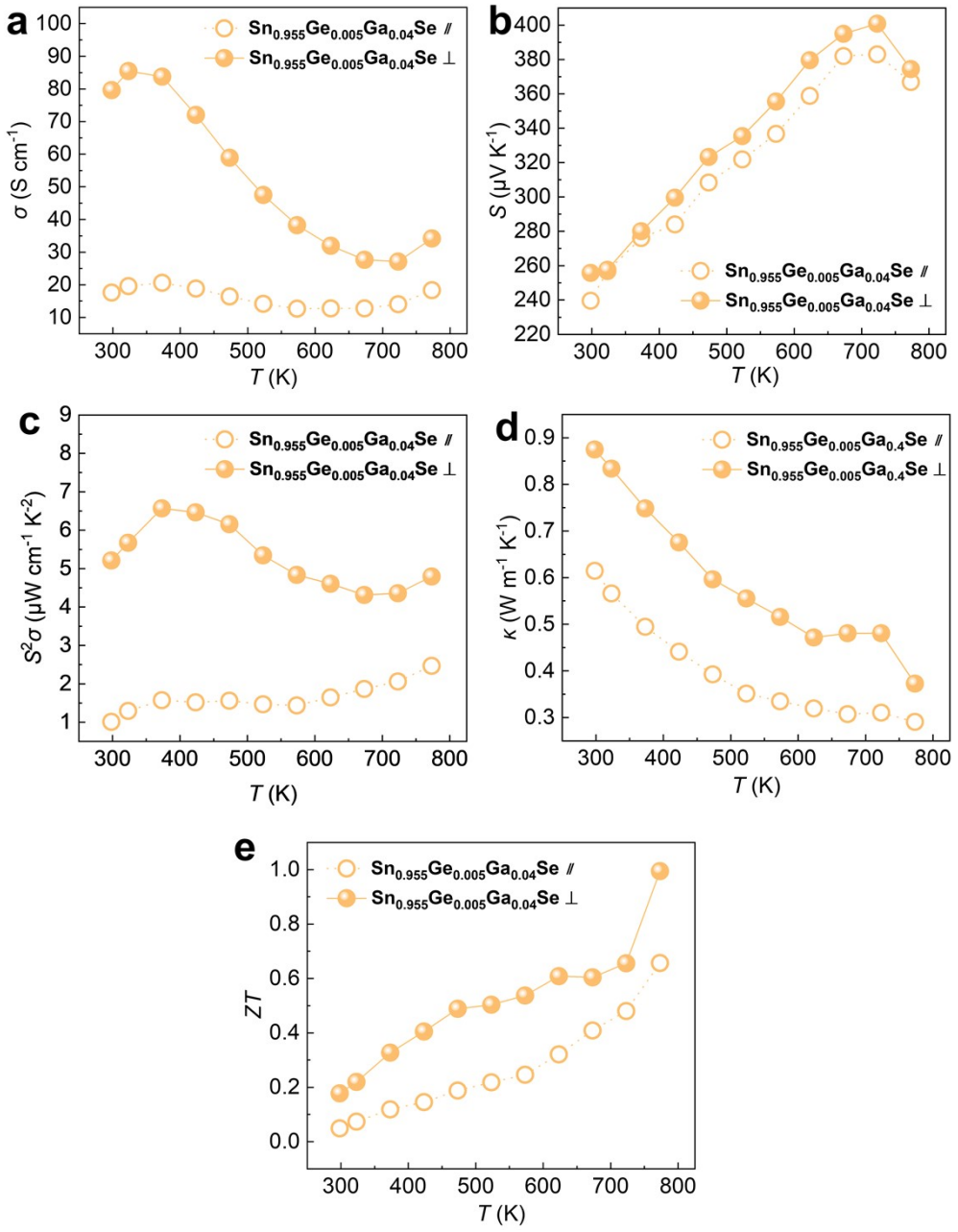

Figure S3. Thermoelectric properties of polycrystalline $Sn_{0.955}Ge_{0.005}Ga_{0.04}Se$ bulk material measured along different directions. Temperature-dependent (a) electrical conductivity (σ), (b) Seebeck coefficient (S), (c) power factor ($S^2\sigma$), (d) thermal conductivity (κ), and (e) ZT value.

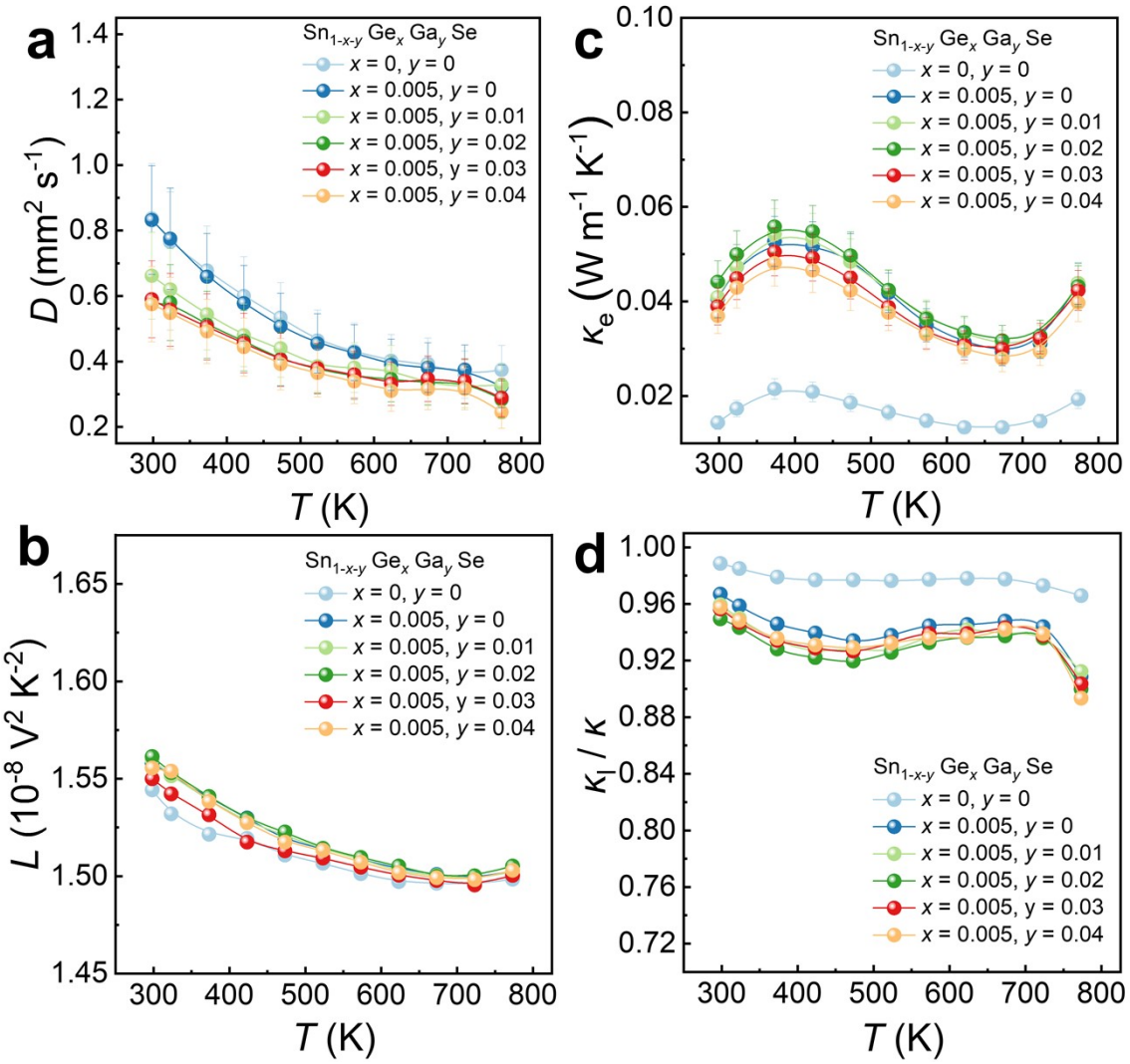

Figure S4. Temperature-dependent properties of polycrystalline $Sn_{1-x-y}Ge_xGa_ySe$ (x = 0, 0.005; y = 0, 0.01, 0.02, 0.03, and 0.04) bulk materials. (a) Thermal diffusivity (D), (b) Lorenz number (L), (c) electronic thermal conductivity (κ_e), and (d) ratio of lattice thermal conductivity to total thermal conductivity (κ_l/κ).

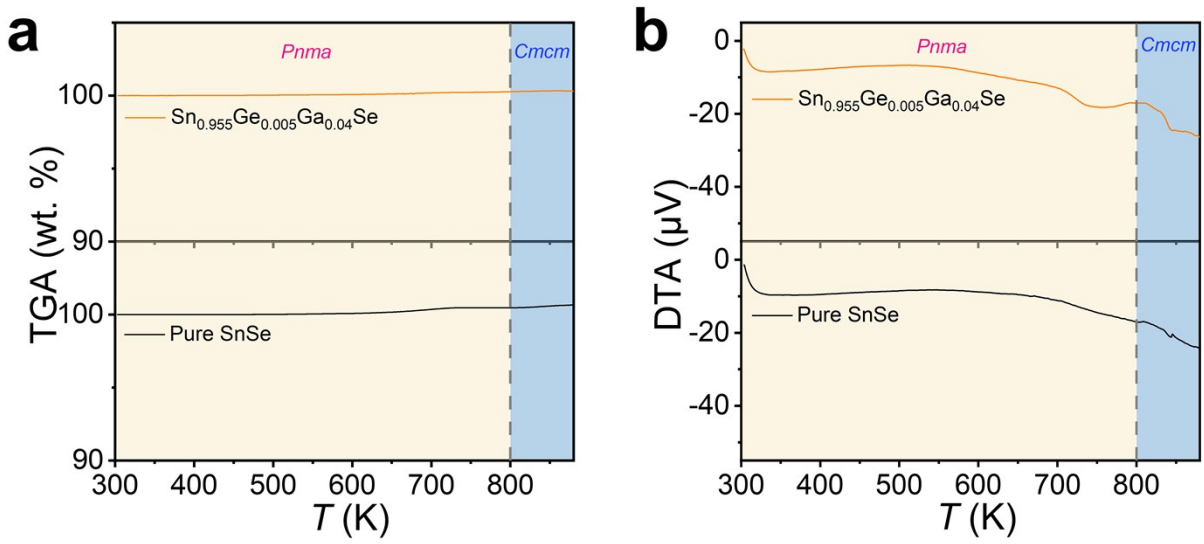

Figure S5. Characterization of the thermal stability of SnSe and $Sn_{0.955}Ge_{0.005}Ga_{0.04}Se$ under argon atmosphere. (a) Thermal gravity analysis (TGA) curves, (b) differential thermal analysis (DTA) curves. Here *Pnma* indicates the low-temperature α-SnSe phase, and *Cmcm* indicates the high-temperature β-SnSe phase.

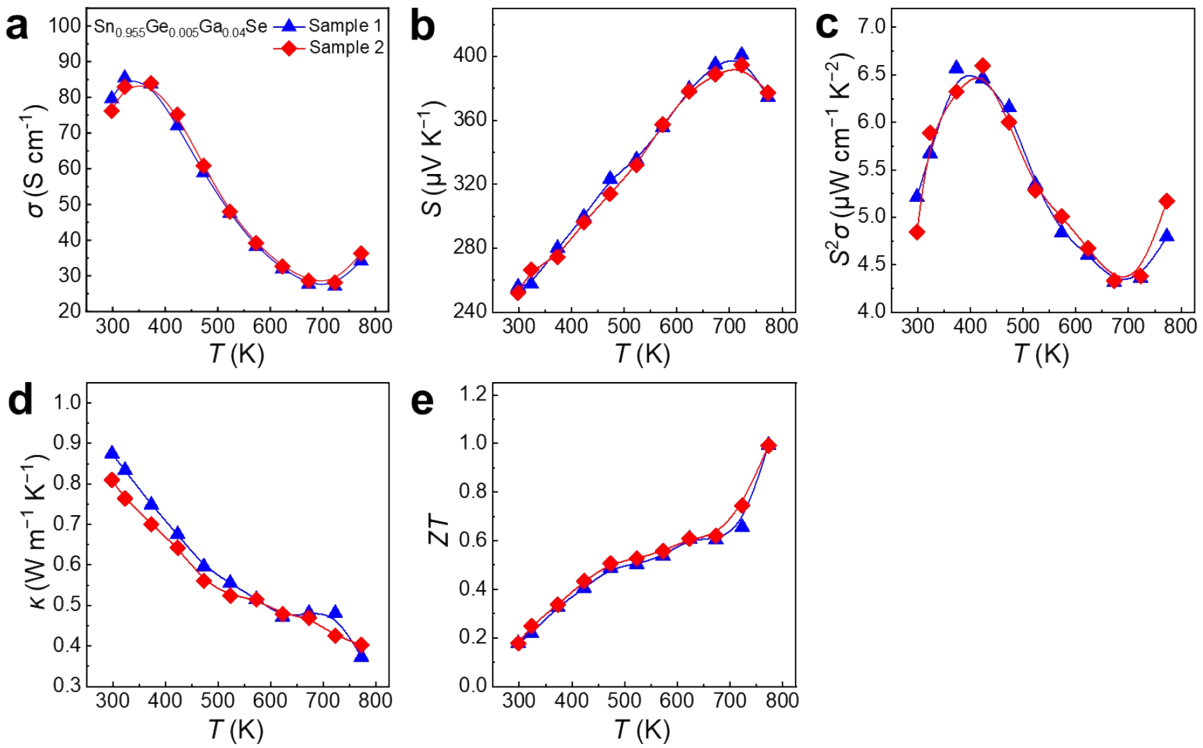

Figure S6. Reproducibility of thermoelectric properties in polycrystalline $Sn_{0.955}Ge_{0.005}Ga_{0.04}Se$ bulk materials. Temperature-dependent (a) σ, (b) S, (c) $S^2\sigma$, (d) κ, and (e) ZT value.

2. Supporting tables.

Table S1 Comparison of defect formation energies in undoped and doped SnSe.

Defect Type	Undoped/eV	Doped/eV	$\Delta E_{(\text{Doped-Undoped})}$
V_{sn}	1.87	1.28	–0.59
Ge_{Sn}	0.58	0.59	+0.01
Ga_{Sn}	0.34	–0.08	–0.42

Table S2. Lattice parameters and unit cell volume of $Sn_{1-x-y}Ge_xGa_ySe$ powders synthesized *via* solvothermal method.

Composition	*a* (Å)	*b* (Å)	*c* (Å)	Unit-cell volume (Å^3)
$x = 0, y = 0$	11.489	4.145	4.440	211.50
$x = 0.005, y = 0$	11.495	4.152	4.4281	211.39
$x = 0.005, y = 0.01$	11.497	4.150	4.429	211.38
$x = 0.005, y = 0.02$	11.489	4.156	4.424	211.30
$x = 0.005, y = 0.03$	11.495	4.149	4.429	211.29
$x = 0.005, y = 0.04$	11.502	4.139	4.433	211.11

Table S3. Mass density (ρ) of $Sn_{1-x-y}Ge_xGa_ySe$ bulk materials. Theoretical density is 6.179 g/cm³.

Composition	ρ (g cm^{-3})	relative ρ (%)
$x = 0$, $y = 0$	5.954	96.36
$x = 0.005$, $y = 0$	5.855	94.76
$x = 0.005$, $y = 0.01$	6.043	97.80
$x = 0.005$, $y = 0.02$	6.023	97.47
$x = 0.005$, $y = 0.03$	6.018	97.39
$x = 0.005$, $y = 0.04$	6.061	98.09

Table S4 Comprehensive comparison of thermoelectric performance in doped polycrystalline SnSe and theoretical predictions.

Material	**Structure**	***ZT***	***T***	***σ***	***S***	***κ***	**ref**
			K	S cm^{-1}	μV K^{-1}	W m^{-1} K^{-1}	
$Na_{0.02}Sn_{0.98}Se$	Polycrystal	0.87	798	56.4	288.8	0.4	[10]
$Na_{0.005}Ag_{0.015}Sn_{0.98}Se$	Polycrystal	0.81	773	60.2	288.2	0.48	[11]
0.1wt% Ag/SnSe	Polycrystal	0.76	773	42.4	307.2	0.42	[12]
$Na_{0.01}Ag_{0.01}Sn_{0.98}Se$	Polycrystal	0.96	673	48.8	348.0	0.44	[13]
$Sn_{0.985}Tl_{0.015}Se$	Polycrystal	0.6	725	77.0	290.2	0.84	[14]
$Sn_{0.94}Bi_{0.06}Se$	Polycrystal	0.21	719	9	−285	0.34	[15]
$Sn_{0.98}In_{0.02}Se$	Polycrystal	0.07	773	6.23	389.6	0.63	[16]
$Sn_{0.98}Pb_{0.02}Se$	Polycrystal	0.6	723	11.04	360.5	0.44	[16]
SnSe	Calculation	1.0	750				[17]
π-SnSe	Calculation	1.20	800				[18]
$Sn_{0.955}Ge_{0.005}Ga_{0.04}Se$	Polycrystal	1	773	34.20	374.44	0.37	**This work**

Reference

1. X.-L. Shi, W.-D. Liu, M. Li, Q. Sun, S.-D. Xu, D. Du, J. Zou and Z.-G. Chen, *Adv. Energy Mater.*, 2022, **12**, 2200670.
2. G. Kresse and J. Hafner, *Phys. Rev. B*, 1994, **49**, 14251-14269.
3. G. Kresse and J. Hafner, *Phys. Rev. B*, 1993, **47**, 558-561.
4. G. Kresse and J. Furthmüller, *Comp. Mater. Sci.*, 1996, **6**, 15-50.
5. G. Kresse and J. Hafner, *J. Phys. Condens. Mat.*, 1994, **6**, 8245-8257.
6. G. Kresse and J. Furthmüller, *Phys. Rev. B*, 1996, **54**, 11169-11186.
7. G. Kresse and D. Joubert, *Phys. Rev. B*, 1999, **59**, 1758-1775.
8. J. P. Perdew, K. Burke and M. Ernzerhof, *Phys. Rev. Lett.*, 1996, **77**, 3865-3868.
9. W. Setyawan and S. Curtarolo, *Comp. Mater. Sci.*, 2010, **49**, 299-312.
10. B. Cai, J. Li, H. Sun, P. Zhao, F. Yu, L. Zhang, D. Yu, Y. Tian and B. Xu, *J. Alloys Compd.*, 2017, **727**, 1014-1019.
11. S. Wang, X. Su, T. P. Bailey, T. Hu, Z. Zhang, G. Tan, Y. Yan, W. Liu, C. Uher and X. Tang, *RSC Adv.*, 2019, **9**, 7115-7122.
12. Z. Wang, X. Hu, H. Lyu, M. Liu, Z. Zhang, J. Li, H. He, C. Zhang and Y. Yu, *J. Alloys Compd.*, 2025, **1018**, 179125.
13. A. Golabek, N. K. Barua, L. T. Menezes, E. Niknam, Z. Yang and H. Kleinke, *ACS Appl. Energy Mater.*, 2024, **7**, 11852-11858.
14. V. Kucek, T. Plechacek, P. Janicek, P. Ruleova, L. Benes, J. Navratil and C. Drasar, *J. Electron. Mater.*, 2016, **45**, 2943-2949.

15. S. Chandra, A. Banik and K. Biswas, *ACS Energy Lett.*, 2018, **3**, 1153-1158.

16. N. K. Singh, S. Bathula, B. Gahtori, K. Tyagi, D. Haranath and A. Dhar, *J. Alloys Compd.*, 2016, **668**, 152-158.

17. R. Guo, X. Wang, Y. Kuang and B. Huang, *Phys. Rev. B*, 2015, **92**, 115202.

18. S. U. Rehman, F. K. Butt, Z. Tariq, X. Zhang, J. Zheng, G. Naydenov, B. Ul Haq and C. Li, *Int. J. Energ. Res.*, 2020, **45**, 6369-6382.